Electronic Properties of Organometallic Metal−Benzene Complexes [M_n(benzene)$_m$ (M = Sc−Cu)]

Tsuyoshi Kurikawa, Hiroaki Takeda, Masaaki Hirano, Ken Judai, Tadashi Arita, Satoshi Nagao, Atsushi Nakajima, and Koji Kaya*

Department of Chemistry, Faculty of Science and Technology, Keio University, 3-14-1 Hiyoshi, Kohoku-ku, Yokohama 223-8522, Japan

Received August 31, 1998

Neutral metal−benzene complexes, M_n(benzene)$_m$ (M = Sc to Cu), are produced for all of the 3d transition metals in the gas phase by using the laser vaporization method. These species are characterized by mass spectrometry, photoionization spectroscopy, and chemical probe experiments. Depending on the metal, there are two types of structures for M_n(benzene)$_m$: multiple-decker sandwich structures and metal clusters fully covered with benzene molecules (rice-ball structures). The former sandwich structure is characteristic of the complexes for early transition metals (Sc−V), whereas the latter is formed for late transition metals (Fe−Ni). Electronic structures of M_1(benzene)$_x$ (x = 1, 2) complexes are investigated through systematic measurements of ionization energies (E_i's).

1. Introduction

Metal−ligand molecules have been a subject of many studies in the past decade.[1−6] Especially, complexes of transition metal atoms and benzene molecules have been the focus of this research as basic models for d−π bonding interactions. Although many synthetic experiments have been conducted on novel organometallics in the condensed phase, various environmental factors such as oxidation or reduction of the products make these approaches problematic. Recently, the advent of the laser vaporization method has caused rapid progress in the study of the organometallic clusters in the gas phase, because the gas-phase conditions can overcome the environmental problems mentioned above. The absence of solvent effects makes it possible to obtain fundamental information on the chemical and physical properties of the metal−molecule complexes, and several groups have reported gas-phase studies of metal−benzene complexes. Armentrout and co-workers[7−9] have reported extensive collision-induced dissociation (CID) experiments which have revealed thermochemistry on ML_n^+ complexes, where M and L are a metal atom and a ligand molecule, respectively. By applying the laser vaporization method, Freiser and co-workers[10−13] have performed the CID experiments on the thermochemistry of transition metal benzene complexes. Duncan and co-workers have investigated dissociation processes of metal ion−benzene complexes by laser photodissociation spectroscopy.[14−16] In their experiments, dissociative charge-transfer processes are discussed in detail. Theoretical calculations have also been carried out. Langhoff and co-workers[17] have calculated binding energies for all the 3d transition metal ions (M^+) with benzene (Bz) and have accounted for the effect of the electron correlation between the metal atoms and the ligand. However, almost all these studies have been restricted to small cationic complexes denoted as $M_1(Bz)_x^+$ (x = 1, 2) due to the necessity for mass selection and to simplify calculations.

In recent work, we have successfully synthesized neutral 3d transition metal−benzene multinuclear complexes by using the molecular beam method for vanadium (V)[18] and cobalt (Co).[19] In this article, through a study of all of the 3d transition metal elements from Sc to Cu, we will present evidence for two different structures of (1) sandwich clusters and (2) rice-ball clusters and discuss their formation mechanism. In addition, we will systematically discuss the periodic trends of ionization energies for the $M_1(Bz)_x$ (x = 1, 2)

(1) Kealy, T. J.; Pauson, P. L. *Nature (London)* **1951**, *168*, 1039.
(2) Miller, S. A.; Tebboth, J. A.; Tremaine, J. F. *J. Chem. Soc.* **1952**, 632.
(3) Muetterties, E. L.; Bleeke, J. R.; Wucherer, E. J.; Albright, T. A. *Chem. Rev.* **1982**, *82*, 499.
(4) *Comprehensive Organometallic Chemistry*; Wilkinson, G., Stone, F. G. A., Abel, E. W., Eds.; Pergamon: New York, 1982; Vols. 3−6.
(5) Wadepohl, H. *Angew. Chem., Int. Ed. Engl.* **1992**, *31*, 247.
(6) Braga, D.; Dyson, P. J.; Grepioni, F.; Johnson, F. G. *Chem. Rev.* **1994**, *94*, 1585.
(7) Ervin, K. M.; Armentrout, P. B. *J. Chem. Phys.* **1985**, *83*, 166.
(8) Chen, Y.-M.; Armentrout, P. B. *Chem. Phys. Lett.* **1993**, *210*, 213.
(9) Meyer, F.; Khan, F. A.; Armentrout, P. B. *J. Am. Chem. Soc.* **1995**, *117*, 9740.
(10) Jacobson, D. B.; Freiser, B. S. *J. Am. Chem. Soc.* **1984**, *106*, 3900.
(11) Hettich, R. L.; Jackson, T. C.; Stanko, E. M.; Freiser, B. S. *J. Am. Chem. Soc.* **1986**, *108*, 5086.
(12) Hettich, R. L.; Freiser, B. S. *J. Am. Chem. Soc.* **1987**, *109*, 3537.
(13) Afzaal, S.; Freiser, B. S. *Chem. Phys. Lett.* **1994**, *218*, 254.
(14) Willy, K. F.; Cheng, P. Y.; Bishop, M. B.; Duncan, M. A. *J. Am. Chem. Soc.* **1991**, *113*, 4721.
(15) Willy, K. F.; Yeh, C. S.; Robbins, D. L.; Duncan, M. A. *J. Am. Chem. Soc.* **1992**, *96*, 9106.
(16) Yeh, C. S.; Willy, K. F.; Robbins, D. L.; Duncan, M. A. *Int. J. Mass Spectrom. Ion Processes* **1994**, *131*, 307.
(17) Bauschlicher, C. W., Jr.; Partridge, H.; Langhoff, S. R. *J. Phys. Chem.* **1992**, *96*, 3273.
(18) Hoshino, K.; Kurikawa, T.; Takeda, H.; Nakajima, A.; Kaya, K. *J. Phys. Chem.* **1995**, *99*, 3053.
(19) Kurikawa, T.; Hirano, M.; Takeda, H.; Yagi K.; Hoshino, K.; Nakajima, A.; Kaya, K. *J. Phys. Chem.* **1995**, *99*, 16429.

10.1021/om9807349 CCC: $18.00
Publication on Web 03/17/1999

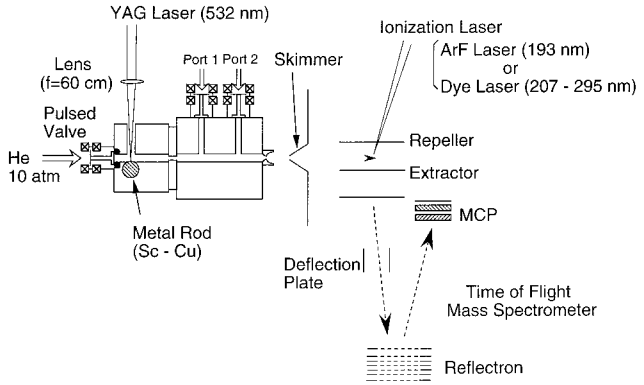

Figure 1. Schematic of an experimental setup. Port 1: benzene diluted with He. Port 2: reaction gas (CO or NH_3) diluted with He.

complexes. Some of these results have been reported previously.[20] This work in the gas phase demonstrates the potential for the synthesis of these novel network organometallic clusters.

2. Experimental Section

Transition metal−benzene clusters, $M_n(Bz)_m$ (M = 3d transition metal atoms from Sc to Cu), were produced by the combination of the laser-vaporization method and a flow tube reactor (FTR). A schematic diagram of an experimental setup used in this experiment is shown in Figure 1, which is modified from one reported previously.[18−21] First, metal atoms (M) were vaporized using the frequency-doubled output from a Q-switched Nd^{3+}:YAG laser (532 nm, ∼10 mJ/pulse) and were cooled to around room temperature with an expansion of He carrier gas (10 atm stagnation pressure). The laser light was focused with a lens having f = 60 cm onto a rotating and translating metal rod which was purchased except for a manganese (Mn) rod. The Mn rod was prepared electrochemically by the deposition onto a stainless steel rod. After the growth of the clusters in a channel (2 mm diameter and 4 cm length), benzene vapor (∼70 Torr) diluted with He carrier gas (1−2 atm) was injected into the FTR. Metal−molecule binary clusters thus generated were sent into the ionization chamber through a skimmer (3 mm diameter). The clusters were ionized by either an ArF excimer laser (193 nm; 6.42 eV) or the frequency-doubled output of a tunable dye laser pumped by a XeCl excimer laser (308 nm) in a static electric field. The photoions were mass-analyzed by a reflectron time-of-flight (TOF) mass spectrometer. To get information about the structures of the clusters, chemical probe and photoionization spectroscopic methods were employed. The $M_n(Bz)_m$ clusters were further reacted with CO or NH_3 gas inside the second FTR which was mounted downstream from the benzene addition port, and the adduct products were mass-analyzed. In the measurement of the ionization energy (E_i) of the complexes the photon energy was changed at 0.01−0.05 eV intervals in the range 5.99−4.20 eV, while the abundance and composition of $M_n(Bz)_m$ clusters were monitored by the ionization of the ArF laser. Fluences of both the dye laser and the ArF laser were monitored by a pyroelectric detector (Molectron J-3) and were kept at ∼200 μJ/cm^2 to avoid multiphoton processes. To obtain photoionization efficiency (PIE) curves, the ion intensities by the second harmonic of the tunable UV dye laser (I_{dye}) were plotted as a function of photon energy (ν) with normalization to both the laser fluence (F_{dye} and F_{ArF}) and the ion intensities by the ArF ionization (I_{ArF}). Then, the normalized ion intensity, $I(\nu)$, is obtained at each photon energy as follows:

$$I(\nu) = \frac{I_{dye}}{F_{dye}} \frac{F_{ArF}}{I_{ArF}} \quad (1)$$

PIE curves were obtained by changing the photon energy in the range 5.99−4.20 eV, and E_i's the clusters were determined from the linear extrapolation of the final decline of PIE curves. The typical uncertainty of the E_i's was estimated to be ±0.05 eV. Some of the PIE curves have been already reported for $M_1(Bz)_2$ (M = Ti, V, and Cr).[21] Dissociation energies (D_0's) were evaluated by using these E_i values, along with known D_0 values for the corresponding cationic complexes.[9,17]

3. Results and Discussion

3.1. Geometrical Structures and Ionization Energies. Figures 2a−i show typical mass spectra resulting from ArF laser ionization of the $M_n(Bz)_m$ (M = 3d transition metals of Sc−Cu) clusters produced by the foregoing procedure. The features of mass spectra will be discussed in the following four parts: (a) Sc−V, (b) Cr−Mn, (c) Fe−Ni, and (d) Cu.

3.1.a. Sc, Ti, and V. The mass spectra of early transition metal−benzene complexes (Sc,[20] Ti,[21] and V[18]) are shown in Figure 2a−c. Prominent peaks in each spectrum occur at almost the same compositions, denoted as $M_n(Bz)_{n+1}$ [henceforth (n, n+1)], although the production efficiency for larger complexes depends on the metal elements. The prominent peaks of (n, n+1) remained unchanged in the mass spectrum, even if (1) the concentration of benzene vapor was increased and (2) CO reactant was also introduced. These results indicate that all the metal atoms of (n, n+1) are contained within the interior of the complexes, because exterior metal atoms should react with CO. Furthermore, when the concentration of metal vapor was increased, minor peaks denoted as (n, n) and (n+1, n) appeared in the spectrum, but there were no peaks for (n+2, n). These two kinds of clusters of (n, n) and (n+1, n) showed adsorption reactions with CO, resulting in (n, n) + 3CO and (n+1, n) + 6CO for V−Bz. These results from the chemical probe experiments indicate that the $M_n(Bz)_{n+1}$ clusters (M = Sc, Ti, and V) are sandwich clusters in which metal atoms and benzene molecules alternate in position. Namely, the superfluous metal atom(s) over the (n, n+1) composition are exterior atoms located at the end of the cluster. These (n, n) and (n+1, n) clusters can reasonably be attributed to sandwich structures having one and two exterior metal atom(s), respectively. Because there are two sites for the exterior atoms, the (n+2, n) cluster is missing. Likewise in the $V_n(Bz)_m$ experiment,[18] the chemical probe experiment leads us to the conclusion that the most likely structure for $Sc_n(Bz)_m$ and $Ti_n(Bz)_m$ clusters is also a multiple-decker sandwich (Figure 3a).[22−26] Very recently, Bowers and co-workers performed ion mobility

(20) Kurikawa, T.; Takeda, H.; Nakajima, A.; Kaya, K. *Z. Phys. D.* **1997**, *40*, 65.
(21) Yasuike, T.; Nakajima, A.; Yabushita, S.; Kaya, K. *J. Phys. Chem. A* **1997**, *101*, 5360.
(22) Salzar, A.; Werner, H. *Angew. Chem., Int. Ed. Engl.* **1972**, *11*, 930.
(23) Duff, A. W.; Jonas, K.; Goddard, R.; Kraus, H.-J.; Krüger, C. *J. Am. Chem. Soc.* **1983**, *105*, 5479.
(24) Lamanna, W. M. *J. Am. Chem. Soc.* **1986**, *108*, 2096.
(25) Li, Q.-S.; Tang, A.-Q. *Sci. China (B)* **1989**, *32*, 897.
(26) Jemmis, E. D.; Reddy, A. C. *Proc. Indian Acad. Sci. (Chem. Sci.)* **1990**, *102*, 379.

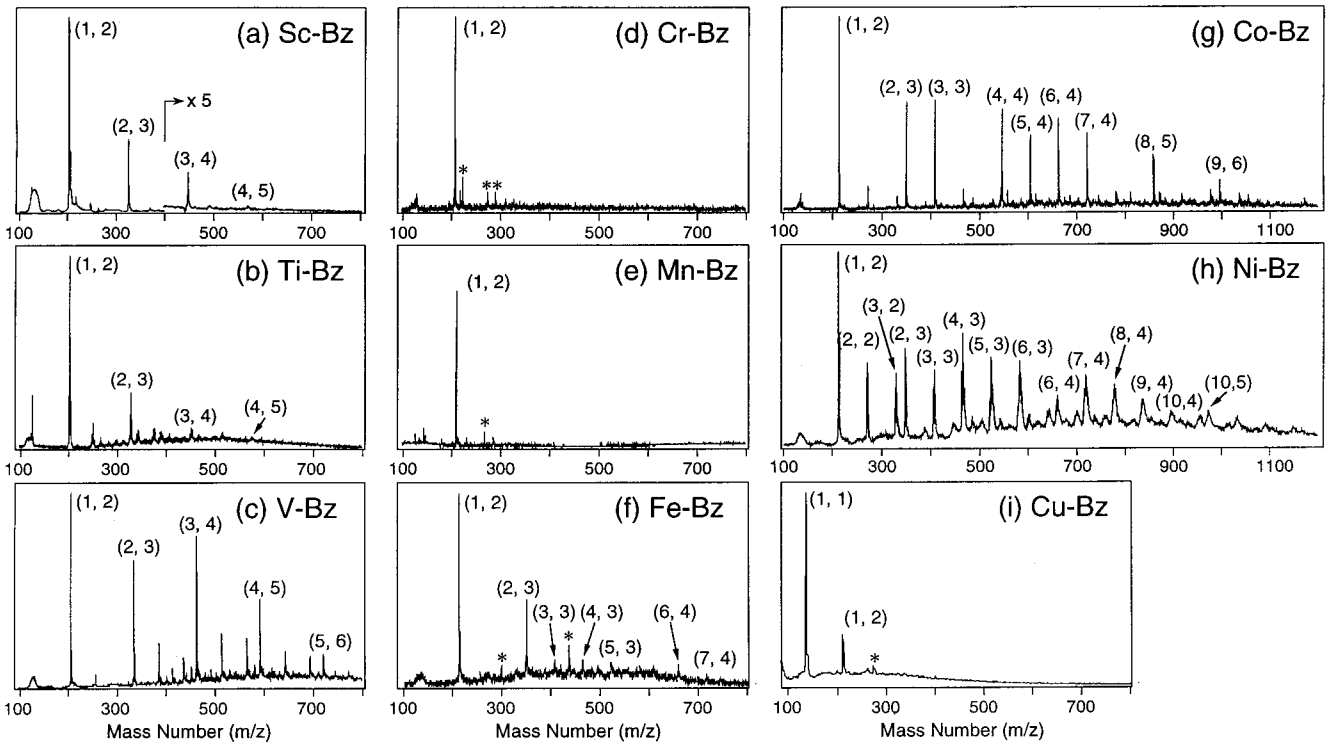

Figure 2. Typical examples of mass spectra of the $M_n(Bz)_m$ complexes (M = 3d transition metals: (a) Sc, (b) Ti, (c) V, (d) Cr, (e) Mn, (f) Fe, (g) Co, (h) Ni, and (i) Cu). $M_n(Bz)_m$ is expressed as (n, m) in the figures, and asterisks (*) denote the contamination peak of oxide.

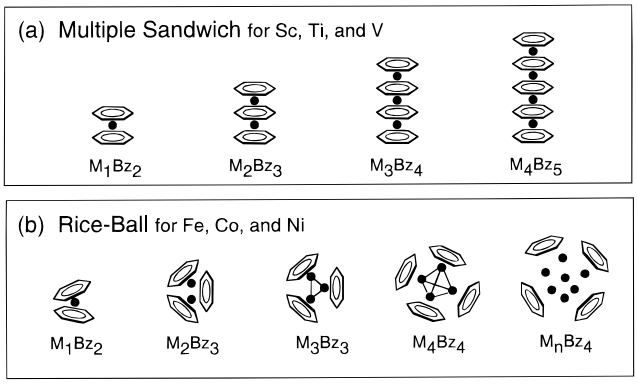

Figure 3. (a) Proposed structures for early transition metals for Sc, Ti, and V; multiple sandwich. (b) Proposed structures for late transition metals from Fe to Ni; riceball.

experiments for the $V_n(Bz)_m$ clusters and reported that they actually exist in the multiple sandwich structure.[27]

The E_i's of $Sc_n(Bz)_m$, $Ti_n(Bz)_m$, and $V_n(Bz)_m$ clusters were measured by the photoionization method, and the values are tabulated in Table 1. Figure 4 shows the E_i values plotted against the number of metal atoms. The E_i values drastically decrease with cluster size n, although the clusters consist of metal atoms and benzenes having relatively high E_i's: E_i(Sc) = 6.54 eV, E_i(Ti) = 6.82 eV, E_i(V) = 6.74 eV, and E_i(Bz) = 9.24 eV.[28] The trend of decreasing E_i is understood as a common feature for the multiple-decker sandwich structure. This phenomenon has been theoretically elucidated[29] by DFT(B3LYP) calculations, showing that the ionization occurs from a delocalized molecular orbital of metal−metal character interposed by the π^* orbitals of benzene. Along the molecular axis of the sandwich cluster, one-dimensional delocalization of the metal dδ(e_{2g}) orbitals occurs through the LUMO (e_{2g}) of C_6H_6, giving a drastic decrease in E_i.

Table 1. Ionization Energies of $Sc_n(Bz)_m$, $Ti_n(Bz)_m$, and $V_n(Bz)_m$ Complexes in eV

	composition		
complexes	n	m	E_i[a]
$Sc_n(Bz)_m$	1	2	5.05(5)
	2	3	4.30(5)
	3	4	3.83(5)
$Ti_n(Bz)_m$	1	2	5.68(4)
	2	3	4.53(5)
	3	4	4.26(5)
$V_n(Bz)_m$	1	2	5.75(3)
	2	3	4.70(4)
	3	4	4.14(5)

[a] The values in parentheses indicate an experimental uncertainty; 5.05(5) represents 5.05 ± 0.05.

To investigate the effect of other aromatic molecules having a η^6 ring, naphthalene (Np) and anthracene (Ant) were reacted with the V vapor instead of Bz, where the symbol η is conventionally used to signify how many carbon atoms of the ring are bonded to the metal atom. A typical mass spectrum of $V_n(Np)_m$ is shown in Figure 5. As found for $V_n(Bz)_m$, prominent peaks in the spectrum are (n, n+1) for n = 1−4, which seems to indicate a series of multiple-decker clusters. In the mass spectrum of $V_n(Np)_m$, however, many minor peaks not

(27) Weis, P.; Kemper, P. R.; Bowers, M. T. *J. Phys. Chem. A* **1997**, *101*, 8207.

(28) (a) Moore, C. E. *Analysis of Optical Spectra*, NSRDS-NBS 34; National Bureau of Standards, 1971. (b) Weast, R. C. *Handbook of Chemistry and Physics*; CRC Press: Boca Raton, 1980, Vol. 61, p E−69. (c) Robinson, J. W. *Handbook of Spectroscopy*; CRC Press: Boca Raton, 1974; Vol. 1, p 257.

(29) Yasuike, T.; Yabushita, S. Submitted to *J. Phys. Chem. A.*

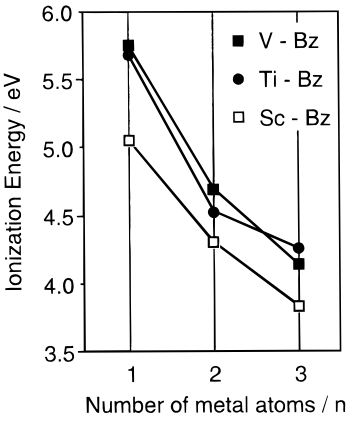

Figure 4. Ionization energies of sandwich complexes of $Sc_n(Bz)_{n+1}$, $Ti_n(Bz)_{n+1}$, and $V_n(Bz)_{n+1}$ plotted against the number of metal atoms from $n = 1$ to 3. (□, Sc−Bz; ●, Ti−Bz; ■, V−Bz).

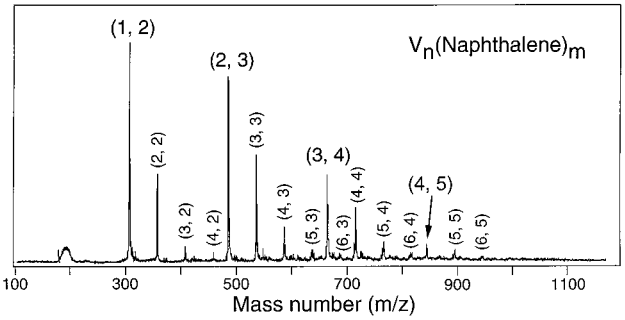

Figure 5. Typical examples of the TOF mass spectra of the $V_n(Np)_m$ clusters. $V_n(Np)_m$ is expressed as (n, m) in the figure.

Table 2. Ionization Energies of $V_1(Bz)_2$, $V_1(Np)_2$, and $V_1(Ant)_2$ Complexes in eV

ligand	E_i[ligand][a]	E_i[V_1(molecule)$_2$][b]
benzene	9.24	5.75(3)[c]
naphthalene	8.13	5.40(5)[d]
anthracene	7.41	5.37(5)[d]

[a] References 28b and 30. [b] The values in parentheses indicate an experimental uncertainty; 5.75(3) represents 5.75 ± 0.03. [c] Reference 18. [d] This work.

corresponding to the $(n, n+1)$ series also appear in the spectrum. Since a naphthalene molecule itself provides four sites on both sides of two η^6 rings, these minor peaks presumably correspond to clusters having exterior metal atoms. For naphthalene and anthracene complexes, the E_i's of $V_1(Np)_2$ and $V_1(Ant)_2$ were determined to be 5.40 ± 0.05 eV [henceforth 5.40(5) eV] and 5.37(5) eV, respectively, as listed in Table 2. Although the E_i's of benzene, naphthalene, and anthracene are 9.24, 8.13, and 7.41 eV, respectively,[28,30] the difference among E_i's of $V_1(Bz)_2$, $V_1(Np)_2$, and $V_1(Ant)_2$ are rather small (E_i-[$V_1(Bz)_2$] = 5.75(3) eV). Thus, it is reasonably presumed that their E_i's are predominantly determined by a local interaction between the d electrons and the π electrons in the sandwich complexes.

3.1.b. Cr and Mn. For Cr and Mn, only the (1, 2) complex was produced (Figure 2d,e). The structure of these clusters is reasonably the sandwich, as reported in the bulk synthesis of $Cr_1(Bz)_2$. It should be noted that the peak intensity of $Cr_1(Bz)_2$ and $Mn_1(Bz)_2$ was relatively small and was estimated to be about 1/10 and 1/200 of $V_1(Bz)_2$, respectively, under similar production conditions. In contrast to the mass spectra of Sc−, Ti−, and V−benzene, the characteristic distribution indicating the multidecker sandwich structure was not seen in the mass spectra of Cr− and Mn−benzene. Although mass spectra were obtained by photoionization of 6.42 eV photon, the absence of the larger clusters is not caused by their high E_i's. There were also no larger clusters in the cations which could be observed with direct extraction into the TOF mass spectrometer without photoionization. As reported previously,[21] the absence of larger clusters can be explained by electron spin restrictions on the growth process. Using the assumption of electron spin conservation, multiple-step nonadiabatic transitions are required to produce the Cr− and Mn−benzene complexes, because the metal−benzene complexes generally prefer to occupy lower electron spin states. This is in contrast to the high electron spin states of the ground state of Cr and Mn atoms. The large difference in electron spin between the product complexes and the reactant metal atoms limits the production of larger clusters. In other words, organometallic complexes of Cr and Mn might be produced efficiently if the electronic excited metal atom having a lower electron spin could be prepared. From the viewpoint of preparing excited-state atoms, the laser vaporization method is promising. The laser plasma makes it possible to prepare various excited metal states without fast relaxation by any environmental factors.

The E_i's of $Cr_1(Bz)_1$, $Cr_1(Bz)_2$, and $Mn_1(Bz)_2$ were obtained as 5.13, 5.43, and 4.28 eV from the measurement of the ionization thresholds. For $Mn_1(Bz)_1$, the E_i could not be measured due to the poor abundance of this complex. The details of these values are discussed later in section 3.2.

3.1.c. Fe, Co, and Ni. Late transition metal-benzene complexes of Fe, Co,[19] and Ni were also produced. Figure 2f−h shows the photoionization mass spectra of $M_n(Bz)_m$ complexes under relatively high concentration of benzene vapor. Even if the concentration of benzene was increased, the mass spectrum remained unchanged. As shown in Figures 2f−h, $M_n(Bz)_m$ clusters exhibit the specific maximum m value (m_{max}) for each n. For Co−Bz, the prominent peaks of (1, 2) and (2, 3) are followed by those of (3, 3), (4, 4), (5, 4), (6, 4), and so on. This behavior in the mass spectrum is completely different from that of the multiple-decker sandwich complexes seen for early transition metals. The $M_n(Bz)_m$ complexes at $n = 3$ and 4, for example, take $m_{max} = 3$ and 4, respectively, while the sandwich complexes take $m = 4$ and 5.

When the magic-number complexes having m_{max} were exposed to the reactant gas NH_3, all of them were unreactive for Fe−Bz, Co−Bz, and Ni−Bz. In contrast to this, other small mass peaks of Co−Bz, such as $(n, m) = (1, 1)$, (2, 2), (3, 2), and (4, 3), are depleted completely by the reaction with NH_3, and instead mass peaks corresponding to the adduct of $Co_n(Bz)_mNH_3$ are formed. This behavior of $Co_n(Bz)_m$ cannot be explained by sandwich structures, because the sandwich complexes with formulas of (3, 3), (4, 4), and so on should

(30) Kimura, K.; Katsumata, S.; Achiba, Y.; Yamazaki, T.; Iwata, S. *Handbook of HeI Photoelectron Spectra of Fundamental Organic Molecules*; Japan Scientific Societies Press/Halsted Press, Tokyo, 1981.

have an exterior Co atom which is expected to react with NH_3. Considering that (1) every number of Co atoms (n) has a specific m_{max} and that (2) they have no exterior Co atoms, the most plausible structure of $Co_n(Bz)_m$ is one with Co_n clusters covered with benzene molecules (m): a rice-ball structure with laver as shown in Figure 3b.[19]

For Ni−Bz, the mass spectrum of $Ni_n(Bz)_m$ complexes was shown in Figure 2h. Although the behavior in the mass spectrum is essentially the same for Co−Bz and Ni−Bz, the Ni−Bz complexes occasionally bind two benzene ligands even under saturation conditions at n = 2, 3, 6, and 10. At $n = 2$, for example, the two peaks of (2, 2) and (2, 3) were observed, and their intensity ratio was almost constant with higher concentration of benzene. Although there is ambiguity of m_{max}, the m_{max} numbers for each n are very similar to those of $Co_n(Bz)_m$. Thus, this behavior seems to indicate that these $Ni_n(Bz)_m$ complexes also take the rice-ball structure in which the Ni_n clusters are fully surrounded by benzene molecules.

For Fe−Bz, peaks denoted as (1, 2) and (2, 3) were mainly observed together with weaker peaks of (3, 3), (4, 3), (5, 3), (6, 4), and (7, 4). As in the cases of Co−Bz and Ni−Bz, it seems reasonable that the peaks of $n \geq 3$ represent a structure fully covered by benzene molecules, i.e., the rice-ball structure, because the patterns in their mass spectra are almost the same.

In this rice-ball structure, m_{max} should be governed by electronic and/or geometric factors. As is well-known in organometallic compounds, an electron counting rule can predict the optimum composition for metal−molecule complexes. Ferrocene [Fe_1(cyclopentadiene)$_2$] and bis(benzene) chromium [$Cr_1(Bz)_2$] are well-known to satisfy an 18-valence-electron (VE) rule. For multinuclear systems, reactions of metal clusters with CO provide useful information on the electronic stability of the clusters.[31−33] In these experiments, a mass-selected metal cluster is reacted with excess CO to determine the saturation coverage. The number of adsorbed CO molecules thus obtained directly reflects the maximum number of VEs that can fill in the valence orbitals of the complex, because CO molecules have essentially no steric interactions with each other. By comparing the number of VEs of carbonyl and benzene clusters, the stability of $M_n(Bz)_m$ clusters can be discussed from an electronic point of view. According to Castleman and coworkers,[31] each Co_n^+ cluster has a maximum number of CO molecules for adsorption. By considering CO and benzene ligands as two- and six-electron donors together with the nine d electrons of the Co atom, the valence electrons of $Co_n(CO)_k^+$ and $Co_n(Bz)_m^+$ cations can be counted as listed in Table 3. In the table, the expected number of benzene ligands, m_E, is also shown, which is estimated from the optimum number of VEs in $Co_n(CO)_k^+$. Without geometrical restrictions, the Co_n^+ cluster would take the corresponding expected number, m_E, of benzene molecules on the basis of the electronic requirement. As cluster size n increases, however, the observed maximum number of added benzenes, m_{max}, starts to become less than the expected one, m_E. Above $n = 6$, the value of m_{max} is 1 or 2 less than m_E. That is to say, the observed $Co_n(Bz)_m^+$ clusters do not necessarily follow the electronic requirement of the metal clusters.

Table 3. Comparison of Total Valence Electrons (VEs) of $Co_n(CO)_k^+$ and $Co_n(Bz)_m^+$ Complexes

$Co_n(CO)_k^+$		expected	$Co_n(Bz)_m^+$	
$(n, k)^+$ [a]	total VEs	number m_E [b]	$(n, m_{max})^+$ [c]	total VEs
$(2, 8)^+$	33	2(3)	$(2, 3)^+$	36
$(3, 10)^+$	46	3(4)	$(3, 3)^+$	45
$(4, 12)^+$	59	4	$(4, 4)^+$	60
$(5, 14)^+$	72	4(5)	$(5, 4)^+$	69
$(6, 16)^+$	85	5(6)	$(6, 4)^+$	78
$(7, 19)^+$	100	6(7)	$(7, 4)^+$	87
$(8, 20)^+$	111	6(7)	$(8, 5)^+$	102

[a] Reference 31. [b] Expected number of benzene molecules, m_E, is obtained from the optimum number of VEs in $Co_n(CO)_k^+$. [c] Observed complexes having the maximum number of benzene, m_{max}.

Table 4. Comparison of Total Valence Electrons (VEs) of $Ni_n(CO)_k^+$ and $Ni_n(Bz)_m^+$ Complexes

$Ni_n(CO)_k^+$		expected	$Ni_n(Bz)_m^+$	
$(n, k)^+$ [a]	total VEs	number m_E [b]	$(n, m_{max})^+$ [c]	total VEs
$(2, 9)^+$	37	3	$(2, 3)^+$	37
$(3, 8)^+$	45	2(3)	$(3, 3)^+$	47
$(4, 10)^+$	59	3(4)	$(4, 3)^+$	57
$(5, 12)^+$	73	4	$(5, 3)^+$	67
$(6, 13)^+$	85	4(5)	$(6, 4)^+$	83
$(7, 15)^+$	99	5	$(7, 4)^+$	93
$(8, 16)^+$	111	5(6)	$(8, 4)^+$	103
$(9, 17)^+$	123	5(6)	$(9, 4)^+$	113
$(10, 18)^+$	135	6	$(10, 5)^+$	129

[a] References 32 and 33. [b] Expected number of benzene molecules, m_E, is obtained from the optimum number of VEs in $Ni_n(CO)_k^+$. [c] Observed complexes having the maximum number of benzene, m_{max}.

For Ni clusters,[32,33] a similar deviation from the expected number of benzene molecules is also seen at large n, which is summarized in Table 4. For Ni−Bz, the value of m_{max} becomes less than that of m_E at n = 5. These results indicate that, as cluster size increases, m_{max} is governed not only by electronic structure but also by the geometry of the corresponding metal cluster (M_n). It is reasonable that the number of benzene molecules is restricted by geometrical factors because steric hindrance between benzene molecules becomes crucial at large n. From the atomic radius of the dimer and the bulk metal,[28b] the radii of Ni_n clusters are presumed to be smaller than those of Co_n clusters. The smaller core of the metal clusters induces the benzene complex to be less stable due to the overlap of benzene molecules at smaller n. This reasonably explains that the deviation for Ni−Bz between m_{max} and m_E is observed at smaller n, compared to Co−Bz.

E_i's of $Co_n(Bz)_m$ and $Ni_n(Bz)_m$ were also measured by the photoionization method, and the values are shown in Figure 6. The E_i's of $Ni_n(Bz)_m$ decrease monotonically as the cluster size n increases, while the E_i's of $Co_n(Bz)_m$ increase at $n \geq 4$. However, both E_i dependences of the cluster size are less sensitive to the cluster size than $V_n(Bz)_m$. This result is reasonably attributed to the differences in their structures; the sandwich structure is prominent for V and the rice-ball structure dominates for Co and Ni. With increasing the cluster size, the

(31) Guo, B. C.; Kerns, K. P.; Castleman, A. W., Jr. *J. Chem. Phys.* **1992**, *96*, 8177.
(32) Fayet, P.; McGlinchey, M. J.; Wöste, L. H. *J. Am. Chem. Soc.* **1987**, *109*, 1733.
(33) Vajda, S.; Wolf, S.; Leisner, T.; Busolt, U.; Wöste, L. H.; Wales, D. J. *J. Chem. Phys.* **1997**, *107*, 3492.

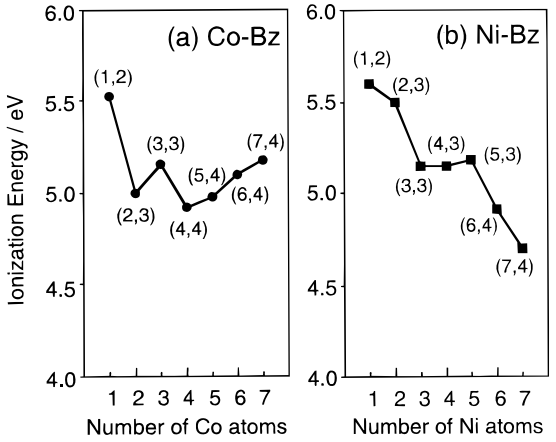

Figure 6. Ionization energies of $Co_n(Bz)_m$ and $Ni_n(Bz)_m$ clusters measured by the photoionization method. The E_i's of $Ni_n(Bz)_m$ decrease monotonically with increasing cluster size n, while the E_i's of $Co_n(Bz)_m$ increase at $n \geq 4$. This result is attributed to the difference in their electronic structures.

sandwich structure makes the 3dδ electrons delocalized along the molecular axis, whereas the rice-ball structure forms only localized d−π interactions at the adsorption sites of benzene. Indeed, the E_i difference between (6, 4) and Co_6 or between (7, 4) and Co_7 is less than 1 eV,[34] which suggests that they have a common framework of the Co_n cluster inside the rice-ball structure.

As for the different E_i's of $Co_n(Bz)_m$ and $Ni_n(Bz)_m$, the energy difference in stabilization between neutrals and cations should be taken into account. The E_i decrease of $Ni_n(Bz)_m$ indicates that the amount of stabilization of neutral $Ni_n(Bz)_m$ clusters is smaller than that of the cationic clusters. On the contrary, the amount of stabilization of neutral $Co_n(Bz)_m$ clusters is larger than that of the cationic clusters. Since the Ni atom has one more VE than Co, the interaction between neutral Ni and benzene should be weaker than that in neutral Co−Bz due to the vacancy for π-electron donation. For their cations, on the other hand, a relatively similar interaction through the positive charge could be expected for both Co−Bz and Ni−Bz cations. Therefore, increasing cluster size n can presumably give less stabilization to $Ni_n(Bz)_m$ clusters than $Co_n(Bz)_m$ clusters. At present, however, a precise description of the molecular orbitals for the rice-ball $M_n(Bz)_m$ is not clear, and careful estimations of molecular orbitals are essential for more detailed discussion.

3.1.d. Cu. For Cu, only the (1, 2) complex was produced, as shown in Figure 2i, and the production efficiency is low. The same pattern is seen for Cr−Bz and Mn−Bz. As shown in the photoionized mass spectrum by the ArF laser, the intensity of (1, 2) is inevitably less than that of (1, 1), although the ionization energies of both species are well below the photon energy, which will be described in the following section. Since there is no electron spin restriction in a growth process for Cu−Bz, the low production efficiency can be ascribed simply to the low binding energy between Cu atoms and benzene molecules. As discussed later, indeed, the binding energy is very low compared to those of other transition metal−benzene complexes. The filled d orbitals in the Cu atom should result in a low binding energy toward benzene molecules because there are no d−π interactions but repulsive interactions between the 4s orbital and the benzene ligand. Then, there is no possibility for multi-Cu metal complexes to grow into the multiple sandwich complexes because the formation of the multiple sandwich structure requires the d−π interaction along the molecular axis. They could, however, grow in the rice-ball structures.

(34) Yang, S.; Knickelbein, M. B. *J. Chem. Phys.* **1990**, *93*, 1533.

Table 5. Ionization Energies of Metal Atoms and $M_1(Bz)_x$ (x = 1, 2) Complexes in eV

M	$E_i[M_1]$[a]	$E_i[M_1(Bz)_1]$[b] this work	$E_i[M_1(Bz)_2]$[b] this work	ref[c]
Sc	6.54	5.07(4)	5.05(5)	
Ti	6.82	5.10(4)	5.68(4)	5.50
V	6.74	5.11(4)	5.75(3)	
Cr	6.77	5.13(4)	5.43(2)	5.45
Mn	7.44		4.28(3)	
Fe	7.87	>6.42	5.18(5)	
Co	7.86	5.55(4)	5.53(3)	
Ni	7.64	5.99−6.42	5.86(3)	
Cu	7.73	5.63(3)	4.30(5)	

[a] Reference 28. [b] The value in parentheses indicates an experimental uncertainty; 5.07(4) represents 5.07 ± 0.04. [c] Reference 35.

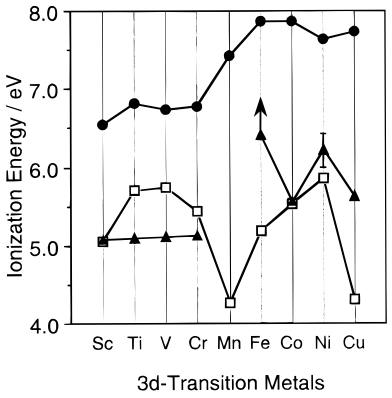

Figure 7. Ionization energies of $M_1(Bz)_x$ (x = 1, 2; M = Sc−Cu) complexes as well as those of metal atoms. (●, E_i's of M_1 [ref 28]; ▲, E_i's of $M_1(Bz)_1$; □, E_i's of $M_1(Bz)_2$). An upward arrow shows that the value shown is the lower limit.

3.2. Ionization Energies and Binding Energies of $M_1(Bz)_x$ (x = 1, 2; M = Sc−Cu). To investigate the electronic properties of $M_1(Bz)_x$ (x = 1 and 2), ionization energies (E_i's) of these complexes were determined by the photoionization method except for that of $Mn_1(Bz)_1$. The results are summarized in Table 5 and are illustrated in Figure 7, including a part of the results that have been reported elsewhere.[20] In some species, the dissociation energies (D_0's) of these neutral complexes could be evaluated, which will be described in section 3.2.c.

3.2.a. E_i's of $M_1(Bz)_1$. From Sc to Cr, an insignificant change is seen in the E_i's of $M_1(Bz)_1$, and this trend shows a striking similarity to the E_i's of the metal atoms, which vary within a narrow range of 0.22 eV. Therefore, it can be expected that the E_i's of $M_1(Bz)_1$ are determined by the energy levels of the corresponding metal atoms. In the ionization of 3d transition metal atoms of Sc−Cr, the ionizing state is the 4s orbital. On the other hand, the highest occupied molecular orbitals (HOMOs) of (1, 1) are metal-originated nonbonding

orbitals described as $3da_1$ under C_{6v} symmetry.[36] Then, it can reasonably be presumed that the ionizing state of $M_1(Bz)_1$ for Sc−Cr is the nonbonding $3da_1$ orbital, which results in the parallelism between E_i's of atom and $M_1(Bz)_1$. The energy level of the nonbonding orbital should be closely related to the atomic energy level.

We could not measure the E_i of $Mn_1(Bz)_1$ because of its poor intensity. Assuming that the HOMO of $Mn_1(Bz)_1$ is described as $3de_1$, which has antibonding character, the generation of $Mn_1(Bz)_1$ produces little bonding stabilization. This is consistent with the fact that the Mn_2 dimer is difficult to produce due to its exceptionally small binding energy (∼200 meV).[37]

Among the benzene complexes for late transition metals Fe, Co, and Ni, only the $Co_1(Bz)_1$ complex has a quite low E_i value. According to the MO diagram for $M_1(Bz)_1$ under C_{6v} symmetry, the HOMO of these complexes is expected to be the same $3de_1$ orbital, which cannot explain this E_i trend. As pointed out by Muetterties et al.,[3] however, partial occupation of electrons in the antibonding $3de_1$ orbital should result in a Jahn−Teller effect, leading to a distortion of the M−(η^6-C_6H_6) fragment to M−η^4 bonding. The reduced symmetry due to this distortion makes the $3de_1$ orbitals separate into stable a′ and unstable a″ orbitals, and thus, the original HOMO of $Co_1(Bz)_1$ with a $3de_1^3$ configuration under C_{6v} symmetry becomes the $(a')^2(a'')^1$ configuration. Then, we can consequently deduce that the electron removal from the $(a'')^1$ configuration will considerably stabilize the $Co_1(Bz)_1^+$ cation, leading to a low E_i of $Co_1(Bz)_1$ compared to the neighboring $Fe_1(Bz)_1$ and $Ni_1(Bz)_1$.

For $Cu_1(Bz)_1$, the E_i value is much less than that of $Ni_1(Bz)_1$. This is probably because the ionization from the HOMO having a $(4sa_1)^1$ configuration gives stability to the corresponding $Cu_1(Bz)_1^+$ cation.

3.2.b. E_i's of $M_1(Bz)_2$. For the (1, 2) complexes from Sc to Cr, theoretical calculations[29] by the DFT(B3LYP) method predict that the ionizing state is the bonding $3de_2$ orbital for Sc, Ti, and V, while it is the nonbonding $3da_1$ orbital for Cr. As the number of bonding electrons in the $3de_2$ orbital increases, the neutral becomes stabilized with respect to the corresponding cation, resulting in the gradual increase of E_i for the (1, 2) complex from Sc to V. When the photoionization efficiency curves of the (1, 2) complex are compared for Sc, Ti, V, and Cr,[29,38] the onset for $Cr_1(Bz)_2$ is the sharpest. This is reasonable because there is little geometric change between the neutral and the cation caused by ionization from the nonbonding $3da_1$ orbital, which is consistent with the theoretical prediction. In case of Mn−Bz, however, the E_i of $Mn_1(Bz)_2$ decreases drastically. This E_i drop can be qualitatively explained by the 18-VE rule. As is well-known for the 18-VE rule, $Cr_1(Bz)_2$ is a very stable complex due to a closed shell electronic configuration. Similar to $Cr_1(Bz)_2$, the electronic configuration of cationic $Mn_1(Bz)_2^+$ is almost the same with 18 VEs. Therefore, we can regard $Mn_1(Bz)_2^+$ with 18 VEs as a stable complex. On the other hand, neutral $Mn_1(Bz)_2$ has 19 VEs. Since the $3de_1$ HOMO of the neutral $Mn_1(Bz)_2$ is expected to be antibonding, occupation of this orbital by one electron offers little energetic advantage. Thus, the E_i of $Mn_1(Bz)_2$ is extremely small compared to values for the other complexes.

In the late transition metals, the E_i of the (1, 2) complexes increases slightly from Fe to Ni, although the E_i's of the corresponding metal atoms are almost the same. Moreover, the differences between the E_i values of the (1, 2) complexes and those of the atoms are rather drastic compared to those for the early transition metal complexes. Although this trend cannot be explained only on the basis of the atomic energy levels, the E_i change is seemingly related to both/either the d−π interaction and/or further structural changes in the (1, 2) complexes. Considering each C_6H_6 ligand as a six-electron donor, together with the valence electrons of the metal atom, the total number of valence electrons in $Fe_1(Bz)_2$, $Co_1(Bz)_2$, and $Ni_1(Bz)$ are 20, 21, and 22, respectively. These (1, 2) complexes are reasonably expected to have sandwich-like structures. As pointed out by Lauher et al.,[39] the HOMO of sandwich complexes having 19−22 valence electrons corresponds to an MO with e_1 symmetry, and this orbital is energetically stabilized by bending the relative orientation of the two benzenes. Since the lower MOs become unstable with the bending angle, the bending configuration is likely to be preferable where the stabilization of the HOMO is compensated by the destabilization of the lower MOs. As the number of electrons increases in the e_1 HOMO, that is from Fe to Ni, the bending angle is expected to become larger. Then, the ionization energy should follow the change in the bending angle as well as the change in the strength of the d−π interaction. In fact, the onset of the photoionization efficiency curves is very gradual compared to those for the early transition metal−benzene complexes, which may indicate that the low-frequency vibration of a bending mode is simultaneously excited upon the ionization of (1, 2).

The E_i of $Cu_1(Bz)_2$ is comparatively small among the late transition metal complexes. This can reasonably be attributed to the highly lying $4sa_1$ HOMO, which originates from the diffuse 4s orbital.

3.2.c. D_0 of $M_1(Bz)_1$ and $M_1(Bz)_2$. To investigate dissociation energies (D_0's), we have to discuss the electron multiplicity of the transition metal−benzene complexes. Although a transition metal atom itself prefers a high electron-spin configuration due to spin−spin exchange interactions, organometallic transition metal complexes, such as metal−benzene, generally take a low electron-spin configuration. This is because a ligand field removes the degeneracy of the d orbitals of the organometallic complexes. There have been no experimental reports on the electron spin of metal atom complexes in the gas phase, but we can deduce their electron spin in some cases, by comparing the experimental results in the gas phase to those in bulk. Ionization energies are a good indicator of the electron spin. For (1, 2) complexes such as $Ti_1(Bz)_2$ and $Cr_1(Bz)_2$, when we compare the E_i value in this work with those

(35) Mingos, D. M. P. In *Comprehensive Organometallic Chemistry; The Synthesis, Reactions and Structures of Organometallic Compounds*; Sir Wilkinson, G., Stone, F. G. A., Abel, E. W., Eds.; Pergamon Press: New York, 1982; Vol. 3, p 29.

(36) Elian, M.; Chen, M. M. L.; Mingos, D. M. P.; Hoffman, R. *Inorg. Chem.* **1976**, *15*, 1148.

(37) Kant, E. A.; Lin, S.-S.; Strauss, B. *J. Chem. Phys.* **1968**, *49*, 1983.

(38) Kurikawa, T.; Nakajima, A.; Kaya, K. Unpublished results.

(39) Lauher, J. W.; Hoffman, R. *J. Am. Chem. Soc.* **1976**, *98*, 1729.

of vapor obtained from bulk complexes, they are in agreement with each other as listed in Table 5. This means that the products of the gas-phase reactions take the same spin state as the bulk complexes. Electron spin of the complexes in the electronic ground state has been investigated by EPR or ESR measurements[40−43] for several species of $V_1(Bz)_1$, $V_1(Bz)_2$, $Cr_1(Bz)_2$, $Ti_1(Bz)_2^+$, $V_1(Bz)_2^+$, and $Cr_1(Bz)_2^+$; their electron spin multiplicities are 2, 2, 1, 2, 3, and 2, respectively. These complexes actually prefer lower electron-spin state as the ground state, but they are not necessarily the lowest multiplicity, and there have been no reports on the electron spin of the other species.

According to quantum chemical calculations for neutral and cationic transition metal−benzene complexes,[17,44−46] many of the (1, 1) and (1, 1)$^+$ complexes still prefer higher electron-spin state. Bauschlicher and co-workers have calculated that the spin multiplicity for the ground state of $V_1(Bz)_1^+$ cation is 5, although that of the corresponding neutral is determined as 2 experimentally. In this case, the ground sate of the $V_1(Bz)_1^+$ cation would be inaccessible by the photoionization of $V_1(Bz)_1$ due to the selection rule for the electron multiplicity of $\Delta S = 1$.

Dissociation energies (D_0's) of the neutral $M_1(Bz)_x$ (x = 1 and 2) complexes were evaluated, from the observed E_i values of $M_1(Bz)_x$ (x = 1, 2; M = Sc−Cu) combined with the known dissociation energies of $M_1(Bz)_x^+$ (x = 1, 2)[9,17] and the E_i's of the metal atoms and neutral $M_1(Bz)_x$ (x = 1 and 2). The evaluation procedure for D_0[M−Bz]and D_0[MBz−Bz] is expressed by following thermochemical cycles:

$$D_0[\mathrm{M-Bz}] = E_i[\mathrm{MBz}] + D_0[\mathrm{M-Bz^+}] - E_i[\mathrm{M}] \quad (2)$$

$$D_0[\mathrm{MBz-Bz}] = E_i[\mathrm{MBz_2}] + D_0[\mathrm{MBz^+-Bz}] - E_i[\mathrm{MBz}] \quad (3)$$

where D_0[M−Bz] (D_0[MBz−Bz]) and D_0[M−Bz$^+$] (D_0[MBz$^+$ −Bz]) are the sequential dissociation energy of the M−Bz (MBz−Bz) neutral and the MBz$^+$ (MBz$^+$−Bz) cation, respectively. However, it is impossible to evaluate the D_0 value reasonably when the ground state of the cation is inaccessible from the neutral, because the E_i value never corresponds to the energy difference between the ground states of the neutral and the cation. $V_1(Bz)_1$ is an example of this case, as mentioned above. Among all of $M_1(Bz)_1$ and $M_1(Bz)_2$, we can conclude that the neutral complexes of $Sc_1(Bz)_1$, $Ti_1(Bz)_1$, $Cu_1(Bz)_1$, and $Cu_1(Bz)_2$ are feasible for the application of this evaluation procedure without ambiguity for electron spin. Their D_0's are tabulated in Table 6. $D_0[Sc_1Bz_2]$ cannot be determined at the present stage, not because of ambiguity for electron spin, but because of the unknown cationic $D_0[ScBz^+-Bz]$. The D_0 values for cationic $M_1(Bz)_1^+$ and $M_1(Bz)_2^+$ have been measured by collision-induced dissociation (CID) and are distributed from 1.5 to 3 eV.[9] Since interactions induced by the positive charge can generally contribute to the binding energy between the atom and benzene molecule, the D_0 value of the cationic complex is larger than that of the neutral. Indeed, D_0 for neutral $Ti_1(Bz)_1$ is 1.76 eV, while that for $Ti_1(Bz)_1^+$ is 2.68 eV.[9] This difference becomes much larger for Cu−Bz. The D_0's of $Cu_1(Bz)_1^+$ and $Cu_1(Bz)_2^+$ have been reported as 2.26 and 1.61 eV,[9] whereas those for $Cu_1(Bz)_1$ and $Cu_1(Bz)_2$ neutrals are only 0.17 and 0.28 eV, as listed in Table 6. The small dissociation energy for neutral Cu−Bz is attributed to the filled d orbitals in the Cu atom, which is consistent with the low production efficiency of the neutral Cu−Bz complexes.

Table 6. Dissociation Energies of $M_1(Bz)_x$ (x = 1, 2) Complexes[a] in eV

species	electron spin multiplicity: neutral	electron spin multiplicity: cation	D_0[b]
$Sc_1(Bz)_1$	2	3[c]	0.63(26)
$Ti_1(Bz)_1$	5[d]	4[c]	1.76(13)[e]
$Cu_1(Bz)_1$	2	1	0.17(13)
$Cu_1(Bz)_2$	2	1	0.28(20)

[a] Dissociation energies were determined from the observed E_i values of $M_1(Bz)_x$ (x = 1, 2) combined with the known dissociation energies of $M_1(Bz)_x^+$ (x = 1, 2) which were determined by the CID experiments; ref 9. [b] The value in parentheses indicates an experimental uncertainty; 0.64(26) represents 0.64 ± 0.26. [c] Calculation; ref 17. [d] Calculation; ref 21. [e] Since a Ti atom takes a ground state of ^{3}F, the energy difference between Ti(^{3}F) and Ti(^{5}F) was added; $\Delta E[^3F-{}^5F] = 0.81$ eV. Then, D_0 was evaluated by the formula $D_0[\mathrm{Ti-Bz}] = E_i[\mathrm{TiBz}] + D_0[\mathrm{Ti-Bz^+}] - E_i[\mathrm{Ti}] + \Delta E[^3F-{}^5F]$.

4. Conclusion

Organometallic clusters of $M_n(Bz)_m$ (M = 3d transition metals) were synthesized by the reaction between laser-vaporized metal atoms and benzene molecules. Different reactivities of metal clusters M_n selectively produce the multiple-decker sandwich clusters for early transition metals of Sc, Ti, and V and the rice-ball structures for late transition metals from Fe to Ni. The sandwich structure complexes exhibit a rapid E_i decrease with cluster size, which can be rationalized by the delocalization of 3dδ electrons along the molecular axis. In the case of the rice-ball structure complexes, the maximum number of benzene molecules adsorped is determined by the steric hindrance of benzene molecules as well as the number of valence electrons. The E_i's of $M_1(Bz)_x$ (x = 1, 2) are sensitive to the electronic configuration of the complex. Especially for Mn and Cu, the (1, 2) complexes exhibit comparatively low E_i values, which can be explained by the instability of the corresponding neutral complexes. The information on the electronic structures of the organometallic complexes strongly suggests the possibility of a synthetic approach to the novel structures by controlling the reaction dynamics through electron-spin selected chemistry.

Acknowledgment. The authors are very grateful to Prof. S. Yabushita and Mr. T. Yasuike for stimulating discussion on the electronic states of the M−Bz complexes. They are also very grateful to Prof. M. A. Duncan

(40) Andrews, M. P.; Mattar, S. M.; Ozin, G. A. *J. Phys. Chem.* **1986**, *90*, 744.
(41) Mattar, S. M.; Hamilton, W. *J. Phys. Chem.* **1989**, *93*, 2997.
(42) Andrews, M. P.; Mattar, S. M.; Ozin, G. A. *J. Phys. Chem.* **1986**, *90*, 1037.
(43) Cloke, F. G. N.; Dix, A. N.; Green, J. C.; Perutz, R. N.; Deddon, E. A. *Organometallics* **1983**, *2*, 1150.
(44) Bauschlicher, C. W., Jr. *Advances in Metal and Semiconductor Clusters*; JAI Press Inc.: London, 1994; Vol. 2, p 115.
(45) Yasuike, T.; Yabushita. S. Private communication.
(46) Ouhlal, A.; Selmani, A.; Yelon, A. *Chem. Phys. Lett.* **1995**, *243*, 269.

(the university of Georgia) for the correction of the English language. This work is supported by a program entitled "Research for the Future (RFTF)" of the Japan Society for the Promotion of Science (98P01203) and by a Grant-in-Aid for Scientific Research on Priority Areas from the Ministry of Education, Science, Sports, and Culture. One of the authors (TK) expresses his gratitude to the Research Fellowships of the Japan Society for the Promotion of Science for Young Scientists.

OM9807349